Draft version February 21, 2014
Preprint typeset using LaTeX style emulateapj v. 20/04/00

arXiv:1402.5088v1 [astro-ph.GA] 20 Feb 2014

G141.2+5.0, A NEW PULSAR WIND NEBULA DISCOVERED IN THE CYGNUS ARM OF THE MILKY WAY

R. Kothes[1], X.H. Sun[2], W. Reich[3], T.J. Foster[4,1]

Draft version February 21, 2014

ABSTRACT

We report the discovery of the new pulsar wind nebula (PWN) G141.2+5.0 in data observed with the Dominion Radio Astrophysical Observatory's Synthesis Telescope at 1420 MHz. The new PWN has a diameter of about 3.5′, which translates at a distance of 4.0 kpc to a spatial extent of about 4 pc. It displays a radio spectral index of $\alpha \approx -0.7$, similar to the PWN G76.9+1.1. G141.2+5.0 is highly polarized up to 40 % with an average of 15 % in the 1420 MHz data. It is located in the centre of a small spherical HI bubble, which is expanding at a velocity of 6 km s^{-1}. The bubble's systemic velocity is -53 km s^{-1} and could be the result of the progenitor star's mass loss or the shell-type SNR created by the same supernova explosion in a highly advanced stage. The systemic velocity of the bubble shares the velocity of H I associated with the Cygnus spiral arm, which is seen across the 2nd and 3rd quadrants and an active star-forming arm immediately beyond the Perseus arm. A kinematical distance of 4±0.5 kpc is found for G141.2+5.0, similar to the optical distance of the Cygnus arm (3.8±1.1 kpc). G141.2+5.0 represents the first radio PWN discovered in 17 years and the first SNR discovered in the Cygnus spiral arm, which is in stark contrast with the Perseus arm's overwhelming population of shell-type remnants.

Subject headings: ISM: individual objects (G141.2+5.0) — ISM: supernova remnants

1. INTRODUCTION

Pulsar wind nebulae (PWNe) are created by fast spinning neutron stars that produce highly relativistic magnetized particle winds, inflating an expanding bubble, confined by the expanding ejecta of the supernova explosion. Electrons and positrons are accelerated to relativistic speeds at the termination shock and interact with the magnetic field generating a synchrotron emitting nebula, called a pulsar wind nebula.

A PWN is characterized by a central concentration of radio continuum emission that gradually declines to the outer edge, in contrast to the more common shell-type supernova remnants (SNRs), which have a limb-brightened appearance. PWNe typically have flat radio continuum spectra with a spectral index α between 0.0 and -0.3 ($S \sim \nu^{\alpha}$, S: flux density, ν: frequency), although steeper spectra have been observed for PWNe DA495 (Kothes et al. 2008) and G76.9+1.1 (Landecker et al. 1993; Kothes et al. 2006). Many of these PWNe, in particular most of the very bright objects like the Crab nebula and 3C58, do not show an accompanying shell-type SNR. This is very puzzling since typically they are relatively young so that the actual remnant of the supernova should not have dissipated, yet.

The Canadian Galactic Plane Survey (CGPS, Taylor et al. 2003) has portrayed the outer Galactic plane with excellent sensitivity and fidelity to extended emission in radio continuum and HI. These qualities have led to the discovery of 13 supernova remnants (SNRs) over the past 12 years (Kothes et al. 2001; Kothes 2003; Kothes et al. 2005; Tian et al. 2007; Foster et al. 2013; Gerbrandt et al. 2013).

2. OBSERVATIONS AND DATA PROCESSING

Radio continuum observations at 408 MHz and 1420 MHz were obtained with the Dominion Radio Astrophysical Observatory's Synthesis Telescope (ST, Landecker et al. 2000) The main characteristics of this survey are the same as for the CGPS Taylor et al. (2003).

The DRAO ST provides observations of linearly polarized emission at four frequency bands around the HI line to allow precise determination of rotation measures (RMs). Those bands are 7.5 MHz wide with center frequencies at 1406.9 MHz (band A), 1413.8 MHz (band B), 1427.4 MHz (band C), and 1434.3 MHz (band D).

Angular resolution varies slightly across the final maps as cosec(Declination). At the centre of G141.2+5.0 the resolution in the final maps is $56'' \times 48''$ (DEC × R.A.) for 1420 MHz continuum, $68'' \times 58''$ for HI, and $3\farcm2 \times 2\farcm8$ for 408 MHz continuum. The RMS noise in the final images is 180 μJy/beam for the 1420 MHz continuum data, 2 K T_b for the HI data, and 2 mJy/beam for the 408 MHz data.

3. RESULTS

3.1. *G141.2+5.0 in Radio Continuum*

The newly discovered extended radio continuum source G141.2+5.0 is shown in Figure 1 in total power. For comparison, we also display images from the Westerbork Northern Sky Survey (WENSS) at 327 MHz (Rengelink et al. 1997) and the VLA Low-Frequency Sky Survey Redux (VLSSr) at 74 MHz (Lane et al. 2012). In the 1420 MHz image, with the best image quality and resolution, this source appears as a diffuse extended radio source with a bright compact core. It is somewhat elon-

[1]National Research Council of Canada, Herzberg Programs in Astronomy and Astrophysics, Dominion Radio Astrophysical Observatory, P.O. Box 248, Penticton, British Columbia, V2A 6J9, Canada
[2]Sydney Institute for Astronomy, School of Physics, The University of Sydney, NSW 2006, Australia
[3]Max-Planck-Institut für Radioastronomie, Auf dem Hügel 69, 53121, Bonn, Germany
[4]Department of Physics and Astronomy, Brandon University, 270 18th Street, Brandon, MB R7A 6A9, Canada

gated along R.A. and has a length of 3.′5 and a height of 3′.

For the radio spectrum determination we use the catalogue flux density at 232 MHz from the Miyun 232 MHz survey (Zhang et al. 1997), where G141.2+5.0 is not resolved. The flux density at 5 GHz was determined with the SPECFIND cross identification catalogue (Vollmer et al. 2010). For the other surveys the flux density has been integrated in concentric rings starting at the radio peak of the source at 1420 MHz ($\alpha_{\rm J2000} = 3^{\rm h}37^{\rm m}12.6^{\rm s}$, $\delta_{\rm J2000} = 61°53'5''$). We used this approach rather than simply using the catalogued fluxes, because sources are typically fitted with a Gaussian model, which may not describe a resolved source very well.

In Figure 1 a small extension from the source to the north is apparent, most likely an unrelated, extragalactic steep-spectrum source. It is obvious from the images in Figure 1 that this source becomes more dominant for longer wavelength. In the DRAO ST and the WENSS images it is clearly a weak insignificant object, but in the VLSSr image it becomes a bright source with significant flux contribution. We fitted a Gaussian to this point source in the 1420 MHz maps and the WENSS data to determine its spectrum (Fig. 3). We removed its contribution from the integrated flux densities of the extended source.

The final flux densities are listed in Table 1 and the integrated radio continuum spectrum of G141.2+5.0 is displayed in Figure 3. We found a straight spectrum between 74 MHz and 5 GHz with a spectral index of $\alpha \approx -0.7$.

3.2. *Polarization Properties of G141.2+5.0*

The polarization image of G141.2+5.0 is shown in Figure 2. In polarization, similar to total power, it has a compact bright core, but its peak is offset from the total power peak and it is elongated north-south. There are two faint arc-like features on either side of the core visible in polarized intensity.

The integrated polarized flux in the DRAO ST observations is $S_{PI} = 18 \pm 3$ mJy. This results in a total fractional polarization of 15 % at 1420 MHz. The peak polarization is more than 40 %.

Since the DRAO ST provides observations of linearly polarized emission at four frequency bands we are able to calculate RMs. In our observations of G141.2+5.0 only the polarized core is sufficiently bright to have a large enough signal-to-noise ratio in the individual bands. In Figure 3, we provide a RM spectrum for this central core. The resulting Faraday rotation is $RM = -101 \pm 9\,{\rm rad\,m^{-2}}$. G141.2+5.0 is listed in the NVSS rotation measure catalogue (Taylor et al. 2009) with an RM of $-37.8 \pm 16.0\,{\rm rad\,m^{-2}}$. However, Taylor et al. (2009) just took the RM at the location of the total power peak of each source. In the case of G141.2+5.0, which is an extended source in the NVSS, there is a strong gradient in polarized intensity (see Figure 2), making this value unreliable.

From our data alone we cannot distinguish between foreground and internal Faraday rotation. The 3D-models of the Galactic magnetic fields, cosmic-ray, and thermal electrons by Sun et al. (2008) and Sun & Reich (2010) give a foreground rotation measure of $-25\,{\rm rad\,m^{-2}}$ for the direction of G141.2+5.0 and a distance of 4 kpc (see section 4.2), consistent with values found in the NVSS RM catalogue (Taylor et al. 2009) in this area of the Galaxy. This indicates significant internal Faraday rotation for G141.2+5.0.

3.3. *The Environment of G141.2+5.0*

In Figure 4, we display HI images of the area around G141.2+5.0. In the top left panel a large area around G141.2+5.0 is displayed. In the centre a small, narrow ring-like feature is discernable surrounding G141.2+5.0.

In the lower right panel, we zoomed in on this ring-like feature. G141.2+5.0 is located in the centre of a depression, which is in most directions surrounded by a broken HI shell. This HI shell is also visible in the R.A.-v and v-DEC slices displayed in Figure 4 as a distinct feature. The distribution of the HI emission indicates that this HI feature actually is a broken HI shell expanding at a rate of $6 \pm 1\,{\rm km\,s^{-1}}$ as indicated by the dashed white circles. This is probably an old HI bubble that has slowed down to a velocity close to the sound speed of the ambient medium and is therefore breaking up. The systemic velocity can be derived from the circles indicating the extend of the HI structure in the R.A.-v and v-DEC slices to be $-53 \pm 1\,{\rm km\,s^{-1}}$.

4. DISCUSSION

In an ongoing survey of an area in the so-called Fan Region, we have serendipitously discovered a previously unidentified diffuse and extended ($\gtrsim 3'$) radio continuum source G141.2+5.0. The Fan region is a highly linearly polarized feature that extends above the mid-plane from a Galactic Longitude of 130° to just beyond the anti-centre (see Figure 11 in Wolleben et al. 2006). G141.2+5.0 is highly linearly polarized with an integrated fractional polarization of about 15 % and a peak of more than 40 %. It shows a steep radio continuum spectrum with a spectral index of $\alpha \approx -0.7$.

4.1. *The nature of G141.2+5.0*

We have tried to identify this source in surveys available through the SkyView Virtual Telescope Database[5]. But we found no counterpart outside the long-wavelength radio regime. Since, in particular, we did not find any counterpart in the infrared we can dismiss the possibility that this source may be an HII region or a nearby Galaxy.

One possible explanation we like to briefly discuss is diffuse synchrotron emission related to a Galaxy cluster, like a halo or a relic, even though the HI shell we found seems to locate G141.2+5.0 inside the Milky Way Galaxy.

Ferrari et al. (2008) report that radio haloes are filling the central areas of Galaxy clusters. They have diffuse quite regular structure with very low linear polarization, low radio surface brightness, and very steep radio continuum spectra with $\alpha \lesssim -1.0$. The low fractional polarization and the very steep radio spectra typically found in haloes make this an unlikely explanation for G141.2+5.0. G141.2+5.0 is too bright, highly polarized, and the radio spectrum is too flat.

Ferrari et al. (2008) also discuss that cluster radio relics are generally filamentary features and commonly found in merging clusters mostly related to shocks. They can be

[5]http://skyview.gsfc.nasa.gov/cgi-bin/titlepage.pl

highly linearly polarized at the 10 - 30 % level and are located at the cluster periphery. Similar to the haloes they have steep radio continuum spectra with $\alpha \lesssim -1.0$. Even though some characteristics of relics are similar to those we found in G141.2+5.0, the steep radio spectra and the filamentary structure make it very unlikely that G141.2+5.0 is a radio relic of a Galaxy cluster.

In particular, since the extended radio source G141.2+5.0 seems to be located inside an expanding HI bubble, but also because of the characteristics of its radio continuum emission, the remnant of a supernova is the most likely explanation. While the structure of G141.2+5.0, a central concentration of radio continuum emission that gradually declines to the outer edge, indicates a pulsar wind nebula, the steep radio continuum spectrum is more reminiscent of a shell-type remnant. However, there are examples for steep spectrum pulsar wind nebulae. The PWN DA 495 has a much steeper radio continuum spectrum than G141.2+5.0 beyond its cooling break frequency of 1.3 GHz (Kothes et al. 2008) and the PWN G76.9+1.1 displays a radio continuum spectrum with a spectral index of $\alpha \approx -0.6$ (Landecker et al. 1993; Kothes et al. 2006). In both cases, the steep spectra are explained by aging, although the recent discovery of a very young energetic pulsar in G76.9+1.1 indicates a young age for the PWN (Arzoumanian et al. 2011). Since shell-type remnants are created by the shockwave of the supernova explosion they always are limb-brightened. G141.2+5.0 is well resolved in our data with a diameter of more than 4 beams. If it was a shell-type SNR it would have an emission hole in the center or have an arc-like appearance.

Therefore we conclude that G141.2+5.0 is most likely a newly identified pulsar wind nebula.

4.2. *The distance of G141.2+5.0*

G141.2+5.0 is observed towards $b \simeq +5°$, well above the maximum latitude to which the Perseus arm is traced. Quadrant II Perseus arm H II regions are found with a mean latitude $b = -0.^{\circ}2$, with 34 out of 37 within $|b| < 2°$ and none at $b \gtrsim +3°$ (see catalogue of Foster & Brunt 2013). Further, the systemic velocity of G141.2+5.0 is with -53 ± 1 km s^{-1} significantly more negative than Perseus arm H I ($v_{LSR} \simeq -39$ km s^{-1} in the midplane). Kinematically then, G141.2+5.0 is not within the Perseus arm, but in the Cygnus spiral arm, the next major star-forming arm about 2.5 kpc beyond Perseus up in the warped disc (Foster & Cooper 2010). In Foster & Brunt (2013) five nearby Cygnus arm H II regions (Sh2-192, 193, 196, LBN 676 & Sh2-204) with comparable ℓ, b, v_{LSR} to G141.2+5.0 have a mean distance among them of 3.8±1.1 kpc.

To estimate the distance to G141.2+5.0 we use the H I modelling method of Foster & MacWilliams (2006) to predict the line-of-sight run of velocity with heliocentric distance, that, along with a simple density model of the H I disk, best describes the observed H I profile in this direction. The variation in the fitted parameters among many modelling runs captures the uncertainty in the model and in the distance to the object. We also account for an uncertainty in the H I shell itself of $\Delta v_{LSR} = \pm 3.4$ km s^{-1} (estimated from such shells around H II regions; see Foster & Brunt 2013). The final kinematic distance to G141.2+5.0 is 4.0±0.5 kpc.

G141.2+5.0 is likely the remnant of a massive star that originally formed in the Cygnus arm, an active star-forming arm well populated with bright OB stars (Negueruela & Marco 2003) and H II regions (Kimeswenger & Weinberger 1989). Despite our favourable view no Cygnus arm supernova remnants (including PWNe) have been conclusively identified. G141.2+5.0 thus represents the first.

4.3. *Some characteristics of the PWN G141.2+5.0*

The newly discovered PWN G141.2+5.0 has a diameter of about 4 pc the same as the young PWN 3C 58 (Kothes 2013). There is no published detection of a pulsar nearby, most likely because there has not been a deep survey for pulsars in this area of the Galaxy, yet. G141.2+5.0 adds to the growing number of PWNe that are found without an associated shell-type SNR. Since we still do not know why this is the case, in particular for young PWNe like the Crab nebula and 3C 58, every new discovery will get us closer to finding the solution for this mystery. There are many possible explanations for the lack of a radio shell: low explosion energy, low ambient density, or low ambient magnetic field, to name just a few. Given the stark contrast between the number of shell-type SNRs in the nearby Perseus arm and none identified in Cygnus, the lack of an accompanying radio shell may not be a coincidence, but rather reflective of a different nature of Cygnus arm supernovae and their environments. However, since we have only one example it may just be a coincidence.

G141.2+5.0 is the only member of this group that has a small HI bubble around it. The HI emission of this feature is, with a few Kelvin above the background, very faint and we only were able to detect it, because it is not confused by much other Galactic HI emission. The HI shell has a diameter of about 12′ which translates to 14 pc at a distance of 4 kpc. At this distance the shell contains about 35 $M_{\odot}$ (±50 %) of material, assuming that 10 % of the atoms are helium and the HI gas is optically thin. The low brightness temperature makes this a valid assumption. This would translate to a pre-bubble density of $n_0 \approx 0.8$ cm^{-3}.

If we assume that the HI shell is the missing SNR shell, it would be close to merging with the interstellar medium (ISM) as evident from the low expansion velocity and the fact that it is breaking apart. From Cioffi et al. (1988), assuming solar abundances, we find for a highly evolved SNR:

$$E_0 = 6.8 \times 10^{43} \left[\frac{n_0}{\mathrm{cm}^{-3}}\right]^{1.16} \left[\frac{v}{\mathrm{km\,s}^{-1}}\right]^{1.35} \left[\frac{R}{\mathrm{pc}}\right]^{3.16} = 2.76 \times 10^{47} \text{ erg}, \quad (1)$$

here E_0 is the explosion energy, n_0 the ambient density, v the shock velocity, and R is the radius. The dynamic age of the shell would be about 350,000 years. This is an extremely low value for the explosion energy and a very old SNR (and PWN).

If the HI shell is the stellar wind bubble of the progenitor star, the lack of a shell-type remnant could be explained by assuming that the SNR shock wave did not reach the HI shell, yet, and is still expanding freely into its low density interior. From Weaver et al. (1977), we find a dynamic age for this bubble of about 700,000 years. This is extremely

young and only very few exceptionally massive stars have such a short life. But those stars would produce a massive stellar wind depositing 10^{51} erg and a lot of material into the ISM. However, stellar winds of massive stars have several phases, an early high velocity low-mass-loss wind during their main sequence time and a slow high-mass-loss wind later on. Kothes & Dougherty (2007) found HI structures very similar to the shell we found around G141.2+5.0 in the massive stellar cluster Westerlund 1. They suggested that these consist of recombined material lost by massive stars in a late high-mass-loss wind. The supernova shockwave could have swept up that material into this shell. Again we would need a highly evolved SNR and a low energy explosion.

Given the discussion above, we propose that G141.2+5.0 is a pulsar wind nebula and the HI shell we found around it is the highly evolved shell-type supernova remnant consisting of swept up high-mass-loss wind material ejected by the progenitor star. In this case the progenitor must have been a massive star, probably of O-type.

G141.2+5.0 is only detected at radio frequencies. We did not find a counterpart in publically available X-ray or γ-ray surveys such as the Fermi Survey. This is not untypical for a highly evolved PWN (e.g. Kothes et al. 2008). Pointed follow-up observations with the CHANDRA satellite may provide crucial information in solving the mysteries around this newly discovered PWN.

5. CONCLUSIONS

G141.2+5.0 is a new radio pulsar wind nebula discovered in follow-up observations of the Canadian Galactic Plane Survey, and the first radio PWN discovered since G63.7+1.1 was reported by Wallace et al. (1997) some 17 years ago. The PWN is a resident of the Cygnus arm about 4 kpc away and is the first SNR discovered in that spiral arm. It displays a steep radio continuum spectrum and has a high level of linear polarization. It sits inside an expanding HI shell, which very likely is related to the expanding shell-type remnant of the same supernova explosion at a highly advanced phase of evolution. This may identify pulsar wind nebulae without an accompanying shell-type remnant as the result of a low energy supernova explosion.

The Dominion Radio Astrophysical Observatory is a National Facility operated by the National Research Council Canada. TF thanks the NRCC for support of his sabbatical year at DRAO. XS was supported by the Australian Research Council through grant FL100100114. We thank P. Reich and T. Landecker for careful reading of the manuscript.

REFERENCES

Arzoumanian, Z., Gotthelf, E. V., Ransom, S. M., et al. 2011, ApJ, 739, 39
Cioffi, D. F., McKee, C. F., & Bertschinger, E. 1988, ApJ, 334, 252
Condon, J. J., Cotton, W. D., Greisen, E. W., et al. 1998, AJ, 115, 1693
Ferrari, C., Govoni, F., Schindler, S., Bykov, A. M., & Rephaeli, Y. 2008, Space Sci. Rev., 134, 93
Foster, T. & Cooper, B. 2010, in Astronomical Society of the Pacific Conference Series, Vol. 438, Astronomical Society of the Pacific Conference Series, ed. R. Kothes, T. L. Landecker, & A. G. Willis, 16–+
Foster, T. & MacWilliams, J. 2006, ApJ, 644, 214
Foster, T. J. & Brunt, C. M. 2013, AJ, submitted
Foster, T. J., Cooper, B., Reich, W., Kothes, R., & West, J. 2013, A&A, 549, A107
Gerbrandt, S., Foster, T. J., Kothes, R., Tung, A., & Geisbüsch, J. 2013, A&A, submitted
Higgs, L. A. & Tapping, K. F. 2000, AJ, 120, 2471
Kimeswenger, S. & Weinberger, R. 1989, A&A, 209, 51
Kothes, R. 2003, A&A, 408, 187
Kothes, R. 2013, A&A, 560, A18
Kothes, R. & Dougherty, S. M. 2007, A&A, 468, 993
Kothes, R., Fedotov, K., Foster, T. J., & Uyanıker, B. 2006, A&A, 457, 1081
Kothes, R., Landecker, T. L., Foster, T., & Leahy, D. A. 2001, A&A, 376, 641
Kothes, R., Landecker, T. L., Reich, W., Safi-Harb, S., & Arzoumanian, Z. 2008, ApJ, 687, 516
Kothes, R., Uyanıker, B., & Reid, R. I. 2005, A&A, 444, 871
Landecker, T. L., Dewdney, P. E., Burgess, T. A., et al. 2000, A&AS, 145, 509
Landecker, T. L., Higgs, L. A., & Wendker, H. J. 1993, A&A, 276, 522
Lane, W. M., Cotton, W. D., Helmboldt, J. F., & Kassim, N. E. 2012, Radio Science, 47, 0
Negueruela, I. & Marco, A. 2003, A&A, 406, 119
Rengelink, R. B., Tang, Y., de Bruyn, A. G., et al. 1997, A&AS, 124, 259
Sun, X.-H. & Reich, W. 2010, Research in Astronomy and Astrophysics, 10, 1287
Sun, X. H., Reich, W., Waelkens, A., & Enßlin, T. A. 2008, A&A, 477, 573
Taylor, A. R., Gibson, S. J., Peracaula, M., et al. 2003, AJ, 125, 3145
Taylor, A. R., Stil, J. M., & Sunstrum, C. 2009, ApJ, 702, 1230
Tian, W. W., Leahy, D. A., & Foster, T. J. 2007, A&A, 465, 907
Vessey, S. J. & Green, D. A. 1998, MNRAS, 294, 607
Vollmer, B., Gassmann, B., Derrière, S., et al. 2010, A&A, 511, A53
Wallace, B. J., Landecker, T. L., & Taylor, A. R. 1997, AJ, 114, 2068
Weaver, R., McCray, R., Castor, J., Shapiro, P., & Moore, R. 1977, ApJ, 218, 377
Wolleben, M., Landecker, T. L., Reich, W., & Wielebinski, R. 2006, A&A, 448, 411
Zhang, X., Zheng, Y., Chen, H., et al. 1997, A&AS, 121, 59

APPENDIX

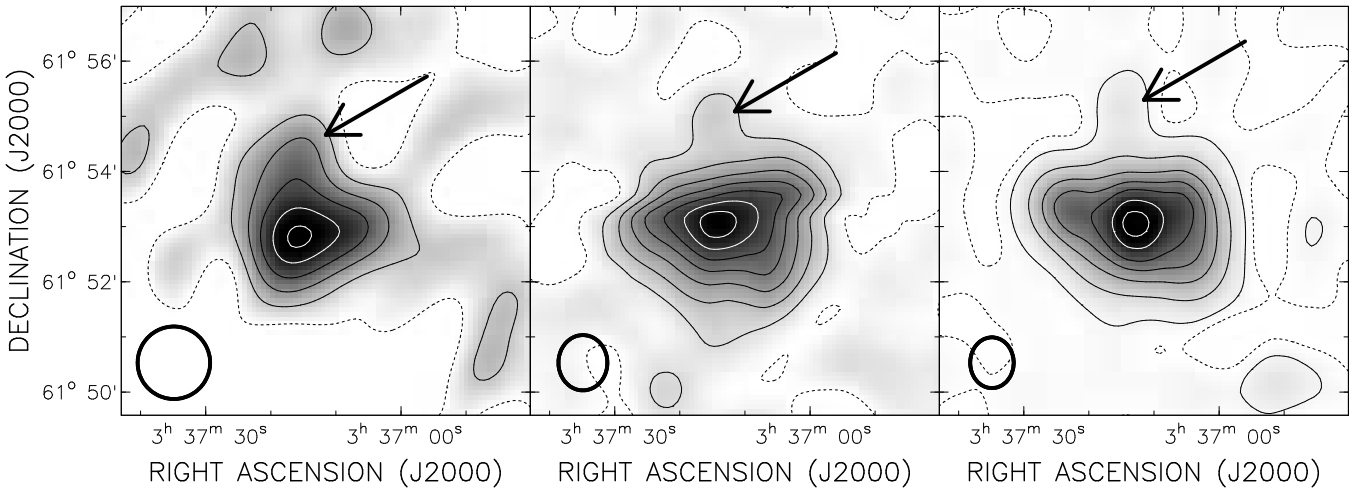

FIG. 1.— Total Power images of the new PWN G141.2+5.0. From the left to the right: VLSS 74 MHz, WENSS 327 MHz, and DRAO ST 1420 MHz. Contours are shown at 100, 200, 300, 400, and 470 mJy/beam at 74 MHz, at 10, 20, 30, 40, 50, 60, and 70 mJy/beam at 327 MHz, and at 1, 4, 8, 12, 16, 22, and 27 mJy/beam at 1420 MHz. The dashed contour indicates the zero level. The angular resolution of the observations is indicated by the circle in the lower left corner. The location of the unrelated point source is indicated by an arrow.

TABLE 1

INTEGRATED FLUX DENSITIES S AT FREQUENCIES ν FOR THE NEWLY DISCOVERED PWN G141.2+5.0. ALL FLUX DENSITIES HAVE BEEN CORRECTED FOR THE CONTRIBUTION OF THE NEARBY POINT-LIKE SOURCE (SEE TEXT).

ν [MHz]	S [mJy]	Reference
74	1100±240	VLSSr (Lane et al. 2012)
151	490±160	7C(G) Survey (Vessey & Green 1998)
232	355±80	Miyun 232 MHz (Zhang et al. 1997)
327	345±100	WENSS (Rengelink et al. 1997)
408	318±35	This paper
1420	137±14	NVSS (Condon et al. 1998)
1420	120±8	This Paper
4850	52±11	SPECFIND Vollmer et al. (2010)

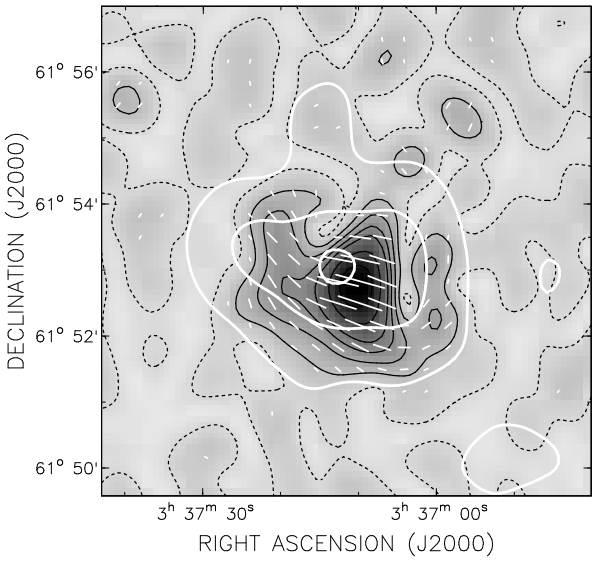

FIG. 2.— Polarized intensity image of the new PWN G141.2+5.0. Black contours are shown at 0.4, 0.8, 1.2, 1.6, 2.4, 3.2, and 4.5 mJy/beam. The dashed contour indicates the zero level. White contours represent the total power emission. Polarisation vectors are overlaid in E-field direction.

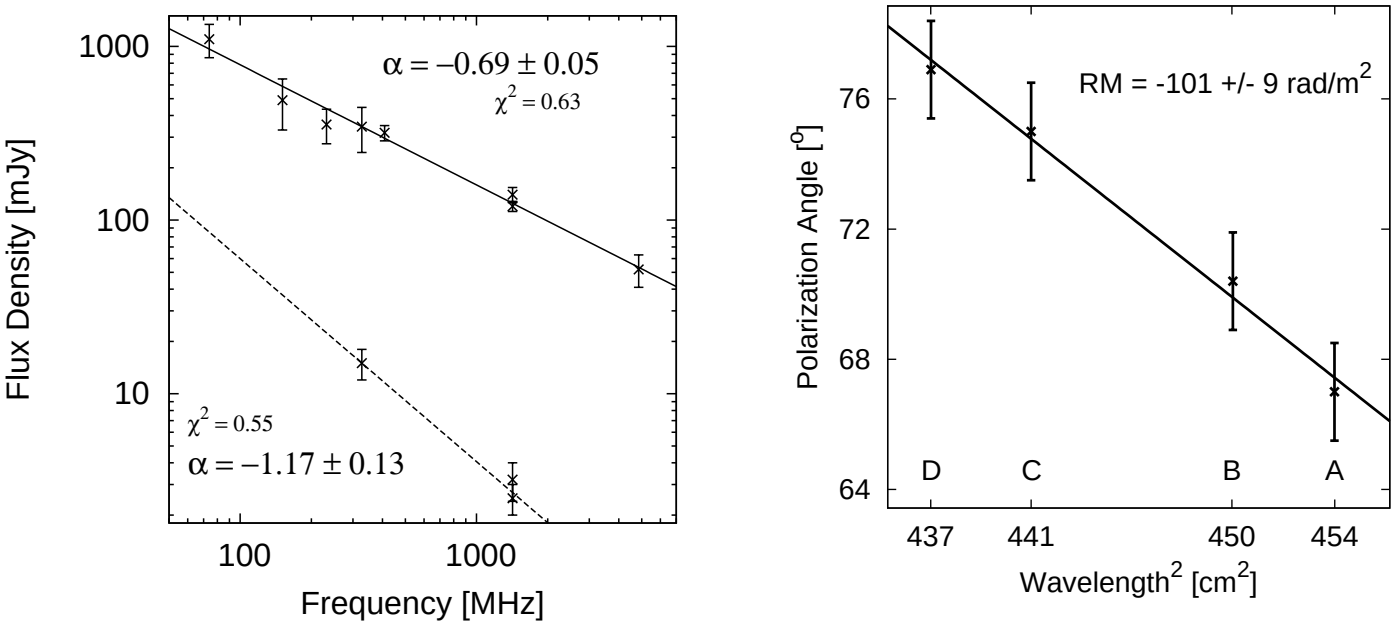

FIG. 3.— Left: Radio continuum spectrum of the new PWN G141.2+5.0 (solid) and the nearby point source (dashed). The spectral indeces and reduced χ^2 are indicated. Right: RM spectrum of the highly polarized core of G141.2+5.0, calculated with the four bands of the DRAO ST observations. The four bands of the DRAO ST observations are indicated.

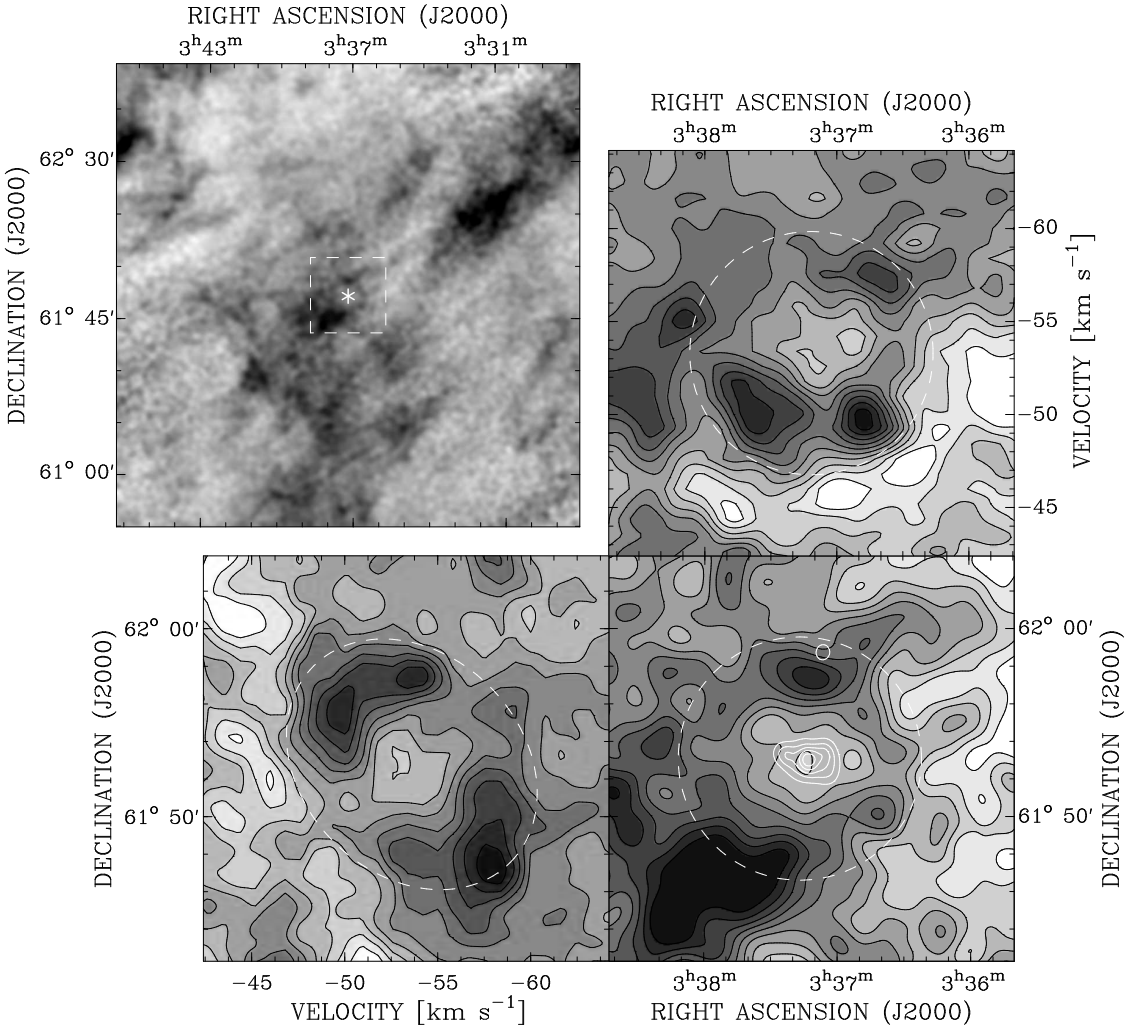

FIG. 4.— HI maps of the area around G141.2+5.0. All images have been convolved to a resolution of 2′. Top left: HI channel map at a radial velocity of about -53 km s^{-1} with single antenna data added taken from the Low-Resolution-DRAO-Survey (LRDS Higgs & Tapping 2000) observed with the DRAO 26 m single antenna telescope. The gray-scale goes from a brightness temperature of 10 K (white) to 40 K (black). The location of G141.2+5.0 is marked by the asterisk. The white box indicates the angular extent of the other three maps. Bottom right: HI channel map at a radial velocity of -53 km s^{-1} zoomed in as indicated by the white box in the top left panel. The radio continuum emission of G141.2+5.0 is indicated by the white contours. Top right: R.A.-velocity representation of the image in the bottom right. Bottom left: Velocity-DEC representation of the image in the bottom right. In all images the dashed circle outlines the putative expanding HI shell.